

Synthesis and H⁺, Cu²⁺, and Zn²⁺ Coordination Behavior of a Bis(fluorophoric) Bibrachial Lariat Aza-Crown

M. Paz Clares,[†] Juan Aguilar,[‡] Ricardo Aucejo,[†] Carlos Lodeiro,[§] M. Teresa Albelda,[†] Fernando Pina,^{*§} J. C. Lima,[§] A. Jorge Parola,[§] João Pina,^{||} J. Seixas de Melo,^{||} Conxa Soriano,[‡] and Enrique García-España^{*†}

Departament de Química Inorgànica ICMOL, Facultat de Química, Universitat de València, Burjassot, Spain, Departamento de Química, REQUIMTE-CQFB, Faculdade de Ciências e Tecnologia, Universidade Nova de Lisboa, Portugal, Departamento de Química ICMOL, Universidade de Coimbra, 3004-535 Coimbra, Portugal, and Departament de Química Orgànica, Facultat Farmàcia, Universitat de València, Burjassot, Spain

Received March 9, 2004

The synthesis, protonation behavior, and Cu²⁺ and Zn²⁺ coordination chemistry of the novel bibrachial aza lariat ether (naphthalen-1-ylmethyl)[2-(20-{2-[(naphthalen-1-ylmethyl)amino]ethyl}-3,6,9,17,20,23,29,30-octazatricyclo-[23.3.1.1*11,15*]triaconta-1(29),11(30),12,14,25,27-hexaen-6-yl)ethyl]amine (**L**) are discussed. The macrocycle, which has two aminoethyl naphthyl moieties symmetrically appended to a 2:2 azapyridinophane structure, displays, in the pH range 2–11, six protonation steps that correspond to the protonation of the secondary amino groups. Steady-state fluorescence measurements show emissions due to the monomer and to the excimer formed between the two naphthalene fragments of the macrocycle. The time-resolved fluorescence data, obtained by the time-correlated single photon counting technique, show that a significant percentage of excimer is preformed as ground-state dimers. The ligand **L** forms with the metal ions Cu²⁺ and Zn²⁺ mono- and dinuclear complexes in aqueous solution. The influence of metal coordination in the fluorescence emission of **L** is analyzed. The acid–base, coordination capabilities, and emissive behavior of **L** are compared with those presented by its synthetic precursor **L1**, which has a tripodal tris(2-aminoethyl)amine structure functionalized at one of its terminal amino groups with a naphthyl moiety.

Introduction

To achieve selective binding of a given guest species and couple the recognition event with a change in a physical property able to signal the process, multifunctional receptors need to be designed and built.¹ Lariat ethers constitute a classical category of receptors in which a macrocyclic structure is covalently linked to appendages containing additional donor atoms. Most lariat ethers are based on crown-ether or oxa-azacrown macrocycles and are designed to complex ammonium cations or spherical metal ions.²

These compounds were born with the idea of joining high thermodynamic stability with fast kinetics to facilitate transport processes through organic membranes. The coordination of the donor atoms in the dangling arms to the metal ion will provide three-dimensionality to the structure preserving at the same time fast coordination dynamics.

To bind transition metal ions, softer atoms should replace the hard ethereal oxygen donors. Nitrogen atoms are appropriate donors for binding divalent first transition metal ions, and new categories of lariat compounds are based on all aza macrocyclic structures.³ Aza macrocycles are, on the other hand, ambivalent receptors since they can coordinate metal ions or anions by simply changing the pH of the medium. If the number of available nitrogen donors is large

* Authors to whom correspondence should be addressed. E-mail: enrique.garcia-es@uv.es (E.G.-E.); fjp@dq.fct.unl.pt (F.P.). Fax: 963544322 (E.G.-E.); 212948550 (F.P.). Tel: 963544879 (E.G.-E.); 212948355 (F.P.).

[†] Facultat de Química, Universitat de València.

[‡] Facultat Farmàcia, Universitat de València.

[§] Universidade Nova de Lisboa.

^{||} Universidade de Coimbra.

(1) (a) Lehn, J. M. *Angew. Chem., Int. Ed. Engl.* **1988**, *27*, 89. (b) Lehn, J. M. *Supramolecular Chemistry. Concepts and Perspectives*; VCH: Weinheim, Germany, 1995.

(2) (a) Gokel, G. W. *Chem. Soc. Rev.* **1992**, *21*, 32. (b) Gokel, G. W.; Barbour, L. J.; De Wall, S. L.; Meadows, E. S. *Coord. Chem. Rev.* **2001**, *222*, 127.

(3) Hartley, J. H.; James, T. D.; Ward, C. J. *J. Chem. Soc., Perkin Trans. 1* **2000**, 3155.

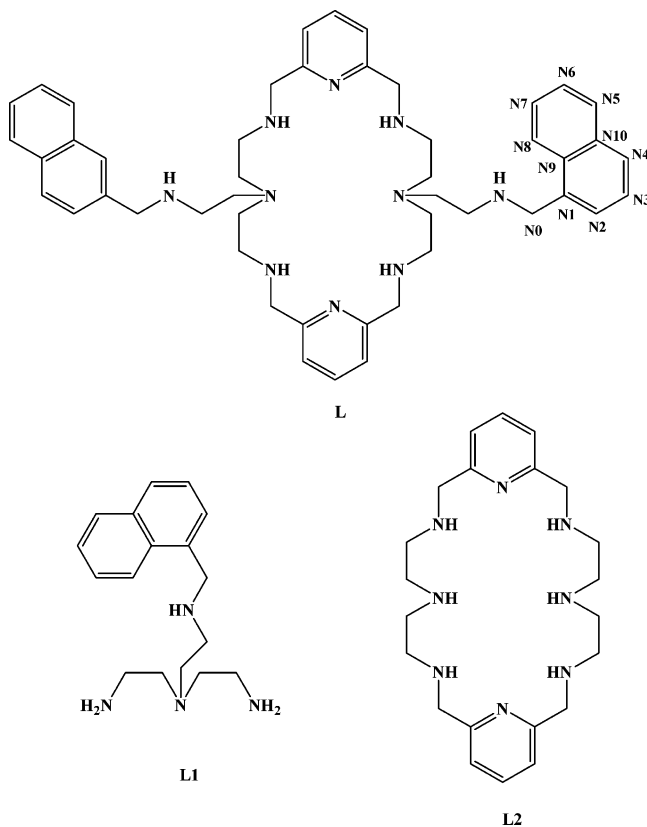
enough they will coordinate metal ions, while if the number and disposition of protonated ammonium sites is adequate, they will be able to coordinate anionic species.⁴ Additionally, if the receptor disposes of subunits displaying physical properties whose magnitudes are largely affected by the interaction with the guest, then the receptor can operate as a molecular sensor.⁵ Polyamine receptors have also constituted the chemical basis of elementary systems, capable of performing simple movements controlled by external inputs (pH, temperature, light, redox potential, metal ions).^{6,7}

Following these ideas, here we report on the receptor **L** in which two aminoethyl naphthyl moieties have been symmetrically appended to a 2:2 azapyridinophane structure (see Chart 1).

This multifunctional receptor meets the characteristics of both the cyclophane and the bibrachial lariat ether receptors.⁸ The nitrogen donors of the macrocycle can be, at least, classified into three categories, secondary and tertiary nitrogens in the bridges and sidearms and the softer pyridine nitrogen donors. The naphthalene rings can contribute to the binding via π -cation interactions and help to signal the encapsulation of a given metal by changing its luminescent behavior. The movements of the pendant sidearms can, on the other hand, give rise to particular emissive properties.⁹

In this first paper concerning the chemistry of **L**, we report on its synthesis and present an overview of its capacity to interact with metal ions. To do so, we have studied the interaction in water of **L** with the divalent metal ions Cu^{2+} and Zn^{2+} . We also report on the fluorescent behavior of the receptor **L** alone and in the presence of the metal ions Cu^{2+} and Zn^{2+} . The acid–base, coordination, and emissive

Chart 1



behavior of **L** is compared with that presented by its synthetic precursor **L1** (see Chart 1), which has a tripodal tris(2-aminoethyl)amine structure functionalized at one of its terminal amino groups with a naphthyl moiety.

Experimental Section

Synthesis of L. Synthesis of L1. Naphthalene-1-carbaldehyde (1.00 g, 6.4 mmol) and N^1,N^1 -bis(2-aminoethyl)ethane-1,2-diamine (2.80 g, 19.2 mmol) were dissolved in 100 mL of EtOH– CH_3CN (1:1). The resulting solution was stirred for 2 h and then the solvent evaporated. The obtained residue was dissolved in EtOH, and NaBH_4 (2.24 g, 59.0 mmol) was added portionwise. After 2 h at room temperature the solvent was evaporated to dryness. The resulting residue was treated with water and repeatedly extracted with dichloromethane (3×50 mL). The organic phase was then dried with anhydrous sodium sulfate and the solvent evaporated to yield the free amine as a yellowish oil. The oil was then taken in a minimum amount of EtOH and precipitated with aqueous HCl as its hydrochloride salt (2.4 g, 93%). Mp: 203–205 °C. ^1H NMR: 2.85 (t, 4H, $J = 6$ Hz), 2.93 (t, 2H, $J = 7$ Hz), 3.09 (t, 4H, $J = 6$ Hz), 3.32 (t, 2H, $J = 7$ Hz), 4.82 (s, 2H), 7.59–7.76 (m, 4H), 8.06–8.16 ppm (m, 3H). ^{13}C NMR: 36.7, 44.3, 48.5, 48.8, 50.1, 122.9, 126.0, 127.1, 127.9, 129.5, 130.1, 131.0, 131.3 ppm. Anal. Calcd for $\text{C}_{17}\text{H}_{29}\text{N}_4\text{Cl}_3$: C, 51.6, H, 7.3, N, 14.1. Found: C, 51.8, H, 7.5, N, 13.9.

Synthesis of (Naphthalen-1-ylmethyl)[2-(20-{2-[(naphthalen-1-ylmethyl)amino]ethyl}-3,6, 9,17,20,23,29,30-octaazatricyclo-[23.3.1.1*11,15*]triaconta-1(29), 11(30),12,14,25,27-hexaen-6-yl)ethyl]amine (L). 2,6-Pyridine-dicarbaldehyde (0.80 g, 5.9 mmol) dissolved in 100 mL was dropwise added to a solution of **L1** (1.7 g, 5.96 mmol) in EtOH and stirred for 2 h. Solid NaBH_4 (1.80 g, 47.4 mmol) was then added portionwise. After 2 h the solvent was

- (4) (a) Dietrich, B. *Pure Appl. Chem.* **1993**, *65*, 1457. (b) Bianchi, A.; Bowman-James, K.; García-España, E. *Supramolecular Chemistry of Anions*; Wiley-VCH: New York, 1997. (c) Beer, P. D.; Gale, P. A. *Angew. Chem., Int. Ed.* **2001**, *40*, 486. (d) Gale, P. A. *Coord. Chem. Rev.* **2001**, *213*, 79. (e) Ilioudis, C. A.; Steed, J. W. *J. Supramol. Chem.* **2001**, *1*, 165.
- (5) (a) Czarnik, A. W. *Fluorescent Chemosensors for Ion and Molecule Recognition*; American Chemical Society: Washington, DC, 1993. (b) Bissel, R. A.; de Silva, A. P.; Gunaratne, H. Q. N.; Lynch, P. L. M.; Maguire, G. E. M.; Sandanayake, K. R. A. S. *Chem. Soc. Rev.* **1992**, 187. (c) de Silva, A. P.; Gunaratne, H. Q.; Gunnlaugsson T.; Huxley, A. J. M.; McCoy, C. P.; Rademacher, J. T.; Rice, T. E. *Chem. Rev.* **1997**, *97*, 1515. (d) de Silva, A. P.; Fox, D. B.; Moody, T. S.; Weir, S. M. *Pure Appl. Chem.* **2001**, *73*, 503. (e) de Silva, A. P.; Fox, D. B.; Moody, T. S.; Weir, S. M. *Trends Biotechnol.* **2001**, *19*, 29. (f) de Silva, A. P.; Fox, D. B.; Huxley, A. J. M.; McClenaghan, N. D.; Roiron, J. *Coord. Chem. Rev.* **1999**, *186*, 297. (g) Kimura, E.; Koike, T. *Chem. Soc. Rev.* **1998**, *27*, 179.
- (6) (a) Kimura, E.; Koike, T. *J. Chem. Soc., Chem. Commun.* **1998**, 1495. (b) König, B.; Pelka, M.; Zieg, H.; Ritter, T.; Bouas-Laurent, H.; Bonneau, R.; Desvergne, J. P. *J. Am. Chem. Soc.* **1999**, *121*, 1681. (c) McLaren, F.; Moore, P.; Wynn, A. M. *J. Chem. Soc., Chem. Commun.* **1989**, 798. (d) Fabbri, L.; Licchelli, M.; Rabaioli, G.; Taglietti, A. *Coord. Chem. Rev.* **2000**, *205*, 85.
- (7) (a) Bernardo, M. A.; Alves, S.; Pina, F.; Seixas de Melo, J.; Albelda, M. T.; García-España, E.; Llinares, J. M.; Soriano, C.; Luis, S. V. *Supramol. Chem.* **2001**, *13*, 435. (b) Albelda, M. T.; Bernardo, M. A.; Díaz, P.; García-España, E.; Seixas de Melo, J.; Pina, F.; Soriano, C.; Luis, S. V. *Chem. Commun.* **2001**, 1520.
- (8) Gatto, V. J.; Arnold, K. A.; Viscariello, A. M.; Miller, S. R.; Gokel, G. W. *Tetrahedron Lett.* **1986**, *27*, 327.
- (9) (a) Bencini, A.; Bianchi, A.; Lodeiro, C.; Masotti, A.; Parola, A. J.; Pina, F.; Seixas de Melo, J.; Valtancoli, B. *Chem. Commun.* **2000**, 1639. (b) Amendola, V.; Fabbri, L.; Mangano, C.; Pallavicini, P. *Struct. Bonding* **2001**, *99*, 79. (c) Parker, D.; Williams, J. A. G. *J. Chem. Soc., Perkin Trans. 2* **1995**, 1305. (d) Beeby, A.; Parker, D.; Williams, J. A. G. *J. Chem. Soc., Perkin Trans. 2* **1996**, 1565.

evaporated to dryness. The residue was treated with water and repeatedly extracted with CH_2Cl_2 (3×40 mL). The organic phase was dried with anhydrous sodium sulfate and the solvent evaporated to dryness to yield an oil (3.3 g, 2.4 mmol, 40%). The oil was then taken in a minimum amount of EtOH and precipitated with aqueous HClO_4 as its perchlorate salt (1.84 g, 31%). Mp: 195–200 °C. ^1H NMR: 2.73–2.73 (m, 2H), 3.00 (t, 2H, $J = 6$ Hz), 3.08 (t, 2H, $J = 7$ Hz), 4.15 (s, 4H), 4.58 (s, 2H), 7.44 (d, 2H, $J = 8$ Hz), 7.54 (t, 1H, $J = 8$ Hz), 7.59 (t, 1H, $J = 8$ Hz), 7.66 (t, 1H, $J = 8$ Hz), 7.66 (d, 1H, $J = 8$ Hz), 7.91 (t, 1H, $J = 8$ Hz), 7.93 (t, 1H, $J = 8$ Hz), 7.97 (d, 1H, $J = 8$ Hz), 8.07 ppm (d, 1H, $J = 8$ Hz). ^{13}C NMR: 43.5, 44.8, 47.8, 48.1, 49.3, 50.9, 122.8, 123.3, 125.8, 126.3, 126.9, 127.7, 129.3, 130.0, 130.8, 131.1, 133.7, 139.6, 150.5 ppm. MS (m/z ; FAB): 779, $[\text{M} + \text{H}]^+$. Anal. Calcd for $\text{C}_{48}\text{H}_{68}\text{N}_{10}\text{Cl}_6\text{O}_{24}$: C, 38.9, H, 4.9, N, 9.8. Found: C, 39.1, H, 4.9, N, 9.5.

Emf Measurements. The potentiometric titrations were carried out at 298.1 ± 0.1 K using 0.15 M NaCl as supporting electrolyte. The experimental procedure (buret, potentiometer, cell, stirrer, microcomputer, etc.) has been fully described elsewhere.¹⁰ The acquisition of the emf data was performed with the computer program PASAT.¹¹ The reference electrode was an Ag/AgCl electrode in saturated KCl solution. The glass electrode was calibrated as a hydrogen-ion concentration probe by titration of previously standardized amounts of HCl with CO_2 -free NaOH solutions and the equivalent point determined by Gran's method,¹² which gives the standard potential, E° , and the ionic product of water ($\text{p}K_w = 13.73(1)$).

The computer program HYPERQUAD was used to calculate the protonation and stability constants.¹³ The pH range investigated was 2.0–11.0, and the concentration of the metal ions and of the ligands ranged from 1×10^{-3} to 5×10^{-3} M with M:L molar ratios varying from 2:1 to 1:2. The different titration curves for each system (at least two) were treated either as a single set or as separated curves without significant variations in the values of the stability constants. Finally, the sets of data were merged together and treated simultaneously to give the final stability constants.

NMR Measurements. The ^1H and ^{13}C NMR spectra were recorded on a Varian UNITY 300 spectrometer operating at 299.95 MHz for ^1H and at 75.43 for ^{13}C . For the ^{13}C NMR spectra, dioxane was used as a reference standard ($\delta = 67.4$ ppm), and for the ^1H spectra, the solvent signal was used.

ROESY (rotating frame spectroscopy) was recorded at three different mixing times, 100, 150, and 600 ms ($\text{pH} = 4$, $T = 298$ K) on a Bruker Avance DPX 500 MHz operating at 500.130 MHz. Adjustments to the desired pH were made using drops of DCl or NaOD solutions. The pD was calculated from the measured pH values using the correlation $\text{pH} = \text{pD} - 0.4$.¹⁴

Diffusion ordered spectroscopy (DOSY)¹⁵ experiments were performed using the bipolar pulse longitudinal eddy current delay (BPPLIED) sequence.

Spectrophotometric and Spectrofluorimetric Titrations. Absorption spectra were recorded on a Shimadzu UV-2501PC spectrophotometer, and fluorescence emissions, on a Horiba-Jobin-Yvon

SPEX Fluorolog 3.22 spectrofluorometer. HCl and NaOH were used to adjust the pH values that were measured on a Meterlab PHM240 Radiometer pH meter. The linearity of the fluorescence emission vs concentration was checked in the concentration range used (10^{-4} – 10^{-6} M). The absorbance of the excitation wavelength was maintained lower than 0.15. When excitation was carried out at wavelengths different from the isosbestic points, a correction for the absorbed light was performed. Fitting of the emission intensity vs [substrate]/[receptor] curves was performed as described in ref 16.

Fluorescence lifetimes were measured with the time-correlated single photon counting technique (TCSPC) as described elsewhere.¹⁶ The fluorescence decays were analyzed using the method of modulating functions implemented by Striker with automatic correction for the photomultiplier "wavelength shift".¹⁷

Results and Discussion

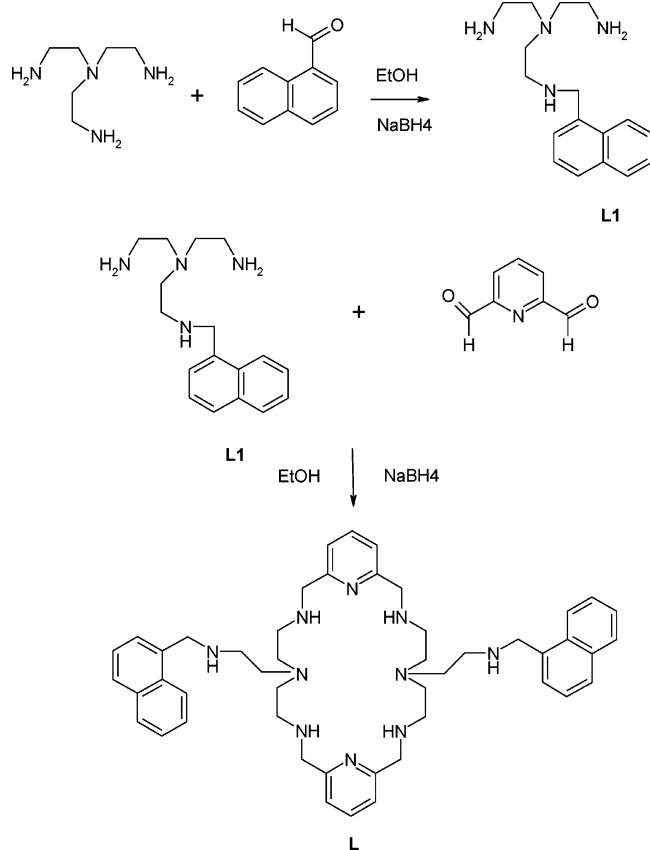
Synthesis. Heteroatomic polyazamacrocycles containing pyridine, pyrazole, furan, and thiophene rings have been obtained by following a two-step synthetic method that consists first of a dipodal (2 + 2) condensation of α,ω -diamines with an aldehyde followed by hydrogenation of the Schiff base imine bonds.¹⁸ By means of this synthetic strategy, we have condensed the polyamine N^1,N^1 -bis(2-aminoethyl)ethane-1,2-diamine (tren) monofunctionalized with a naphthyl group with 2,6-pyridinedicarbaldehyde in ethanol followed by in situ reduction with sodium borohydride (Scheme 1). The global yield of the reaction is high and allows for disposing of gram quantities of the final product that is handled as its hydrochloride or perchlorate salts. The high yield obtained agrees with those usually reported for dipodal (2 + 2) condensation of α,ω -diamines with dialdehydes and is much higher than those reported for amines containing NH groups in the middle of the chain. In such cases, formation of imidazoline rings produces a new isomer which reduces the overall yield of the reaction.¹⁸ In our case, the tertiary nature the middle nitrogens prevents the formation of such imidazoline isomers and facilitates the formation of the 26-membered macrocyclic ring.

Monofunctionalization of tris(2-aminoethyl)amine (tren) was achieved by reacting the free amine with naphthalene-1-carbaldehyde in 3:1 molar ratio followed by treatment with NaBH_4 . The excess of amine is added to ensure predominant formation of the 1:1 functionalized **L1** compound. The excess of amine is removed along the extraction process.

- (10) García-España, E.; Ballester, M. J.; Lloret, F.; Moratal, J. M.; Faus, J.; Bianchi, A. *J. Chem. Soc., Dalton Trans.* **1988**, 1, 101.
 (11) Fontanelli, M.; Micheloni, M. *Proceedings of the 1st Spanish-Italian Congress on Thermodynamics of Metal Complexes*; Diputación de Castellón: Castellón, Spain, 1990.
 (12) (a) Gran, G. *Analyst* **1952**, 77, 881. (b) Rossotti, F. J.; Rossotti, H. J. *Chem. Educ.* **1965**, 42, 375.
 (13) (a) Sabatini, A.; Vacca, A.; Gans, P. *Coord. Chem. Rev.* **1992**, 120, 389. (b) Gans, P.; Sabatini, A.; Vacca, A. *Talanta* **1996**, 43, 1739.
 (14) Convington, A. K.; Paabo, M.; Robinson, R. A.; Bates, R. G. *Anal. Chem.* **1968**, 40, 700.
 (15) Johnson, C. S., Jr. *Prog. NMR Spectrosc.* **1999**, 34, 203.

- (16) (a) Albelda, M. T.; Díaz, P.; García-España, E.; Lima, J. C.; Lodeiro, C.; Seixas de Melo, J.; Parola, A. J.; Pina, F.; Soriano, C. *Chem. Phys. Lett.* **2002**, 353, 63. (b) Pina, F.; Lima, J. C.; Lodeiro, C.; Seixas de Melo, J.; Díaz, P.; Albelda, M. T.; García-España, E. *J. Phys. Chem. A* **2002**, 106, 8207. (c) Seixas de Melo, J.; Pina, F.; Soriano, C.; Parola, A. J.; Lima, J. C.; Albelda, M. T.; Clares, M. P.; García-España, E.; Soriano, C. *J. Phys. Chem. A* **2003**, 107, 11307.
 (17) Striker, G.; Subranariam, V.; Seidel, C. A. M.; Volkmer, A. *J. Phys. Chem. B* **1999**, 103, 8612.
 (18) For related synthesis see for instance: (a) Bailey, N. A.; Eddy, M. M.; Fenton, D. E.; Moss, S.; Mukhopadhyay, A.; Jones, G. *J. Chem. Soc., Dalton Trans.* **1984**, 2281. (b) Chen, D.; Martell, A. E. *Tetrahedron* **1991**, 47, 6895. (c) Dhont, K. I.; Lippens, W.; Herman, G.; Goemine, A. M. *Bull. Soc. Chim. Belg.* **1992**, 101, 1061. (d) Arán, V. J.; Kumar, M.; Molina, J.; Lamarque, L.; Navarro, P.; García-España, E.; Ramírez, J. A.; Luis, S. V.; Escuder, B. *J. Org. Chem.* **1999**, 64, 6135. (e) Menif, R.; Martell, A. E.; Squattrito, P. J.; Clearfield, A. *Inorg. Chem.* **1990**, 29, 4723. (f) Adams, H.; Bailey, N. A.; Fenton, D. E.; Hempstead, P. D.; Westwood, G. P. *J. Inclusion Phenom. Mol. Recognit. Chem.* **1991**, 11, 63.

Scheme 1

**Table 1.** Protonation Constants of the Macrocycles **L**, **L1**, and **L2** Determined in 0.15 M NaCl at 298.1 K

reacn ^a	L	L1	L2^c
$L + H = HL$	9.46(3) ^b	9.72(1)	9.25
$HL + H = H_2L$	8.46(4)	9.10(1)	8.49
$H_2L + H = H_3L$	7.65(5)	7.45(1)	7.55
$H_3L + H = H_4L$	7.25(7)		6.98
$H_4L + H = H_5L$	6.50(5)		4.11
$H_5L + H = H_6L$	6.29(6)		3.26
$6H + L = H_6L$	45.61		39.64

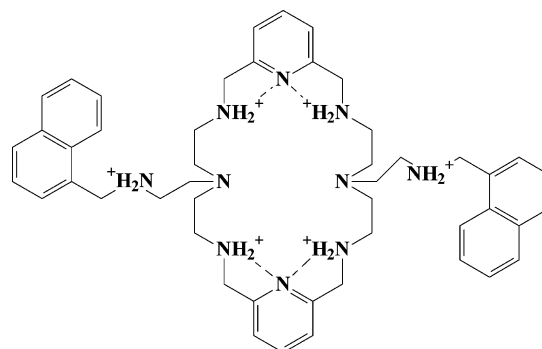
^a Charges omitted for clarity. ^b Values in parentheses are standard deviations in the last significant figure. ^c Taken from ref 18.

Protonation Constants and Effect of the pH on the Emissive Behavior. The protonation constants of **L** determined in 0.15 M NaCl at 298.1 K together with those we have calculated for the tripodal open-chain ligand **L1** and those reported in the literature for the pyridinophane macrocycle **L2** (see Chart 1)¹⁹ are presented in Table 1. The distribution diagram together with the results of steady-state fluorescence titration are shown in Figure 1.

Under the experimental conditions used, **L** displays six measurable protonation steps with values in the range 9.46–6.29 logarithmic units. The protonation constants of the four first steps are comparable to those found for the related monocyclic compound **L2** without the dangling arms. The fifth and sixth protonation constants are clearly higher for **L** than for **L2** in agreement with the possibility that **L** has to dispose the positive charges far away between them in

(19) Lu, Q.; Carroll, R. J.; Reibenspies, J. H.; Martell, A. E.; Clearfield, A. *J. Mol. Struct.* **1998**, 470, 121.

Chart 2



the secondary nitrogen atoms of the macrocycle (See Chart 2). In a similar way, the first three constants of **L** are close although a little lower than those of **L1**. The slightly higher constants of the two first protonation steps of **L1** (Table 1) can be ascribed to the presence of two primary amino groups than can stabilize better their charges by hydrogen bonding with the water molecules of the medium.

In agreement with the behavior found for related ligands reported in the literature,^{19–21} the pyridine nitrogen atoms do not seem to experience any net protonation process in the explored pH range. However, the width of the ¹H and ¹³C signals of protons Hpy0 (for the labeling see Chart 1) suggests that the pyridine nitrogen atoms participate in an intramolecular hydrogen-bonding network. Indeed, at pH 6, the Hpy0 signals very significantly broaden relative to what is found at more acidic pH values. Also the ¹³C NMR signals are much broader at this pH.

The fluorescence emission spectra of compound **L** reported in Figure 1A shows two bands. The first band centered at 323 nm is vibrationally resolved and can be easily assigned to the emission of naphthalene (monomer). The second band at 390–400 nm is much broader and can be assigned to a naphthalene–naphthalene excimer. An analogous spectral pattern has been found for naphthalene derivatives presenting interaction between two chromophores.^{7,16,23,24} Inspection of Figure 1B shows that the H₆L⁶⁺ species exhibits both the most intense monomer and most intense excimer emissions. Removal of the first and successive protons produces a strong quenching due to a photoinduced electron transfer from the lone pairs of the deprotonated amine to the excited naph-

- (20) Bencini, A.; Bianchi, A.; García-España, E.; Micheloni, M.; Ramírez, J. A. *Coord. Chem. Rev.* **1999**, 88, 97.
- (21) (a) Costa, J.; Delgado, R. *Inorg. Chem.* **1993**, 32, 5257. (b) Costa, J.; Delgado, R.; Drew, M. G. B.; Félix, V.; Henriques, R. T.; Warendborough, J. C. *J. Chem. Soc., Dalton Trans.* **1999**, 3253.
- (22) Seixas de Melo, J.; Albelda, M. T.; Díaz, P.; García-España, E.; Lodeiro, C.; Alves, S.; Lima, J. C.; Pina, F.; Soriano, C. *J. Chem. Soc., Perkin Trans. 2* **2002**, 991.
- (23) Albelda, M. T.; García-España, E.; Gil, L.; Lima, J. C.; Lodeiro, C.; Seixas de Melo, J.; Melo, M. J.; Parola, A. J.; Pina, F.; Soriano, C. *J. Phys. Chem. B* **2003**, 107, 6573.
- (24) (a) Fabbri, L.; Poggi, A. *Chem. Soc. Rev.* **1995**, 24, 197. (b) Czarnik, A. W. *ACS Symp. Ser.* **1993**, No. 538, 104. (c) Fabbri, L.; Licchelli, M.; Pallavicini, P.; Perotti, A.; Taglietti, A.; Sacchi, D. *Chem.—Eur. J.* **1996**, 2, 75. (d) Akkaya, E. U.; Huston, M. E.; Czarnik, A. W. *J. Am. Chem. Soc.* **1990**, 112, 3590. (e) Fabbri, L.; Licchelli, M.; Pallavicini, P.; Perotti, A.; Sacchi, D. *Angew. Chem., Int. Ed. Engl.* **1994**, 33, 1975. (f) Czarnik, A. W. *Acc. Chem. Res.* **1994**, 27, 302. (g) Valeur, B.; Leray, I. *Coord. Chem. Rev.* **2000**, 205, 3. (h) Valeur, B.; Pouget, J.; Bourson, J. *J. Lumin.* **1990**, 52, 345.

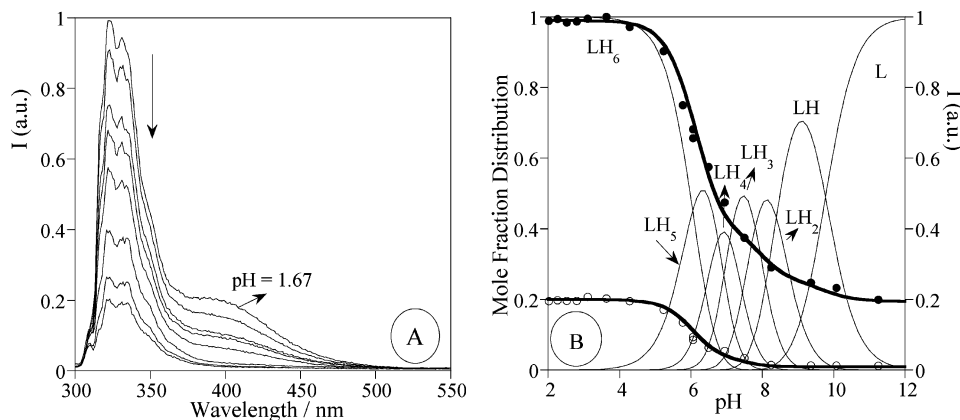


Figure 1. (A) Fluorescence emission spectra of **L** recorded at 298.1 K as function of pH. (pH values: 1.67; 5.23; 5.77; 6.06; 7.07; 7.85; 8.25; 11.25.) (B) Steady-state fluorescence emission titration curves of **L** ($\lambda_{\text{exc}} = 280$ nm) for a 7.01×10^{-6} M solution in 0.15 NaCl at 298.1 K in water: (●) emission followed at 323 nm (monomer); (○) emission followed at 400 nm (excimer); (—) molar fraction distributions.

Table 2. Fluorescence Decay Times, Preexponential Factors and χ^2 Values Resulting from the Global Analysis of the Decays as a Function of pH Obtained with Excitation Wavelength of 290 nm and Emission Wavelengths of 320 and 420 nm

pH	λ_{em}	τ_1/ns	τ_2/ns	τ_3/ns	a_{i1}	a_{i2}	a_{i3}	χ^2
2.1	320	9.8	34		0.917	0.083		0.83
	420				0.319	0.681		1.04
3.13	320	10.87	35.5		0.926	0.074		1.29
	420				0.28	0.716		1.09
4	320	10.75	35.5		0.92	0.08		1.2
	420				0.135	0.861		1.09
5.2	320	13.8	38.33	4.57	0.614	0.046	0.34	0.87
	420				0.196	0.78		1.01

thalene.²⁴ This type of quenching has analogously been observed in other polyamine systems bearing naphthalene or anthracene fluorophores.^{5–7,9,16} While the quenched emission from the monomer still remains above pH = 8, no excimer emission is observed at those pH values. In fact, the excimer emission starts to decrease at pH = 5, coinciding with the formation of H_3L^{5+} and totally disappears at higher pH values.

To get more information about the excimer formation kinetics we have performed a detailed analysis of the fluorescence decays of **L**.

In Table 2, the fluorescence decay times and preexponential factors collected at 320 and 420 nm, at different pH values, are presented. It can be seen that the global analysis of the fluorescence decays leads to biexponential fits until $\text{pH} \cong 4$. From there on, the decays are best fitted with sums of three exponentials.

Note that by direct comparison with Figure 1B, from pH = 2 to 4 the only emitting species are the totally protonated H_6L^{6+} species and an intramolecular excimer. At pH = 5.2, the decays become essentially triexponential at the monomer emission wavelength. The independent analysis of the decays at 420 nm gives rise to biexponential fits with the absence of the shortest component. This new component is totally compatible with the existence, at pH above 5, of two different protonated species (H_6L^{6+} and H_3L^{5+} in Figure 1B) coexisting with the intramolecular excimer. This is also compatible with the fact that H_3L^{5+} does not form excimer, since the decays at 420 nm remain unchanged. As the pH increases, the H_3L^{5+} species gains weight relative to the H_6L^{6+} species (see Figure 1B), which leads to an increase in the associated

Table 3. Stability Constants for the Formation of Cu^{2+} and Zn^{2+} Complexes of the Macrocycle **L** Determined in 0.15 M NaCl at 298.1 K

entry	reacn ^a	Cu(II)	Zn(II)
1	$\text{M} + 3\text{H} + \text{L} = \text{MH}_3\text{L}$	41.18(5) ^b	34.21(2)
2	$\text{M} + 2\text{H} + \text{L} = \text{MH}_2\text{L}$	36.09(7)	28.48(3)
3	$\text{M} + \text{H} + \text{L} = \text{MHL}$	28.97(8)	20.92(6)
4	$\text{M} + \text{L} = \text{ML}$	20.13(9)	11.75(9)
5	$2\text{M} + \text{L} + 2\text{H} = \text{M}_2\text{H}_2\text{L}$	41.3(1)	
6	$2\text{M} + \text{L} + \text{H} = \text{M}_2\text{HL}$	37.97(5)	
7	$2\text{M} + \text{L} = \text{M}_2\text{L}$	31.06(9)	21.14(4)
8	$2\text{M} + \text{L} + \text{H}_2\text{O} = \text{M}_2\text{L}(\text{OH}) + \text{H} + \text{H}$	21.2(1)	12.39(8)
9	$2\text{M} + \text{L} + 2\text{H}_2\text{O} = \text{M}_2\text{L}(\text{OH})_2 + 2\text{H}$	11.47(9)	
10	$\text{MH}_2\text{L} + \text{H} = \text{MH}_3\text{L}$	5.1	5.7
11	$\text{MHL} + \text{H} = \text{MH}_2\text{L}$	7.1	7.6
12	$\text{ML} + \text{H} = \text{MHL}$	8.8	9.2
13	$\text{M}_2\text{HL} + \text{H} = \text{M}_2\text{H}_2\text{L}$	3.5	
14	$\text{M}_2\text{L} + \text{H} = \text{M}_2\text{HL}$	6.9	
15	$\text{M}_2\text{L} + \text{H}_2\text{O} = \text{M}_2\text{L}(\text{OH}) + \text{H}$	−9.9	−8.8
16	$\text{M}_2\text{L}(\text{OH}) + \text{H}_2\text{O} = \text{M}_2\text{L}(\text{OH})_2 + \text{H}$	−10.0	
17	$\text{ML} + \text{M} = \text{M}_2\text{L}$	10.9	9.4

^a Charges omitted for clarity. ^b Values in parentheses are standard deviations in the last significant figure.

preexponential factor of the shortest decay time; see Table 2.

The absence of negative amplitudes associated with the decay times found at 420 nm can be explained by either a strong contribution of the monomer emission at that wavelength (in comparison with the weak excimer emission) and/or to the presence of preformed dimers, that cannot be excluded.

NMR DOSY experiments performed at pH = 6 (Figure S1) show the presence of at least three different conformers of **L** in solution with close diffusion coefficients. The diffusion coefficients obtained together with the dilution experiments performed rule out the possibility of intermolecular aggregation in the concentration range of study. Therefore, the different conformers observed should correspond to intramolecular arrangements with different shape and consequently different hydrodynamic radius.

Interaction with Metal Ions. Table 3 gathers the cumulative and some selected stepwise constants for the interaction of **L** with the metal ions Cu(II) and Zn(II) determined at 298.1 K in 0.15 M NaCl aqueous solutions.

Formation of mono- and dinuclear complexes has been detected in all the studied systems. The mononuclear

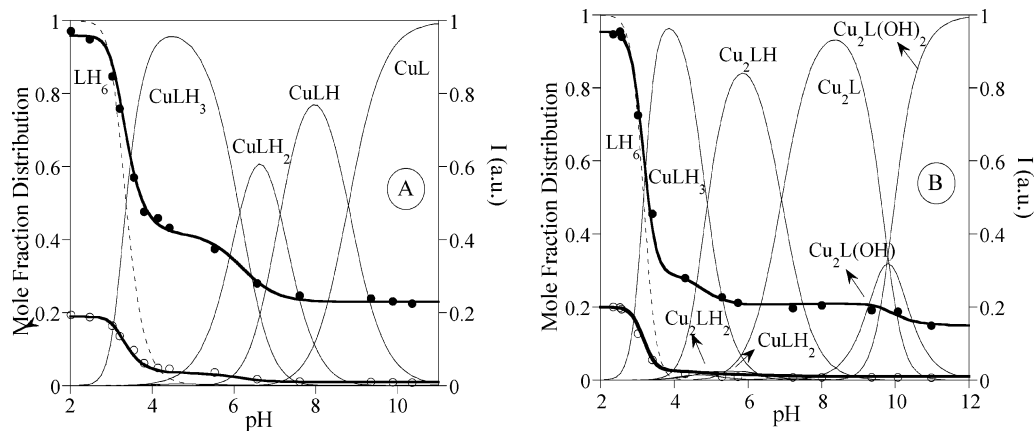


Figure 2. Steady-state fluorescence emission titration curves for the system $\text{Cu}^{2+}-\text{L}$ ($\lambda_{\text{exc}} = 280 \text{ nm}$) for a $7.01 \times 10^{-6} \text{ M}$ of **L** (molar ratio 1:1 **L**:**M** (A) and 1:2 **L**:**M** (B)), with 0.15 M NaCl at 298.1 K in water: (●) emission followed at 323 nm (monomer); (○) excimer emission followed at 400 nm; (free ligand dotted lines and metal complex solid lines) molar fraction distributions.

complexes display $[\text{M}(\text{H}_3\text{L})]^{5+}$, $[\text{M}(\text{H}_2\text{L})]^{4+}$, $[\text{M}(\text{HL})]^{3+}$, and $[\text{ML}]^{2+}$ stoichiometries. The dinuclear Cu^{2+} complexes present $[\text{Cu}_2(\text{H}_x\text{L})]^{(4+x)}$ stoichiometries with x values varying from 2 to -2 . For 2:1 **M**:**L** molar ratios these species predominate throughout all the pH range studied (see Figure 2). For the Zn^{2+} system, only the dinuclear species $[\text{M}_2\text{L}]^{4+}$ and $[\text{M}_2\text{L}(\text{OH})]^{3+}$ are found.

The high values of the protonation constants of the mononuclear complexes (entries 10–12, Table 3) agree with the fact that these protonation processes take place at noncoordinated nitrogen atoms. Indeed, the 10 potential donor atoms existing in the macrocycle exceed the optimal coordination numbers of anyone of these metal ions. The donor atoms can be classified into four categories: (i) the two pyridine nitrogens; (ii) the four secondary amino groups in the polyamine bridges; (iii) the two secondary amino groups of the dangling arms; (iv) the two tertiary central nitrogen atoms of the bridges (see Chart 1 and Scheme 1). Geometrical reasons prevent the simultaneous participation of some of these atoms in the coordination to the same metal ion. For instance, it is unlikely that both pyridine nitrogen atoms can simultaneously get close enough to bind a single metal ion since they lie rather far apart. Molecular models show distances for the separation between the pyridine nitrogens that go over 6.5 Å in all the cases. Moreover, in the crystal structure of the dinuclear $[\text{Cu}_2(\text{L2})](\text{ClO}_4)_4 \cdot 4\text{DMF}$ complex reported by Martell et al.,¹⁹ the larger axis of the macrocyclic hole was that bisecting the opposite pyridine nitrogen atoms. Therefore, the coordination of the first metal ion should involve one of the pyridine nitrogen atoms that as they do not take part neatly in protonation processes, will have their lone pair always available for the coordination and the amino nitrogen atoms close to it. Such a coordination was also the one observed in each one of the two coordination sites of the solid complex $[\text{Cu}_2(\text{L2})](\text{ClO}_4)_4 \cdot 4\text{DMF}$.¹⁹ The number of nitrogen atoms involved in the coordination deserves, however, further analysis. In this sense although, as is correctly stated, deriving coordination numbers just from free energy terms can be very misleading, in some instances a careful comparison with appropriate systems can provide good hints at this respect. The reported values for the

Table 4. Stability Constants for the Formation of Cu^{2+} and Zn^{2+} Complexes of the Tripodal Ligand **L1** Determined in 0.15 M NaCl at 298.1 K

entry	reacn ^a	Cu(II)	Zn(II)
1	$\text{M} + \text{H} + \text{L} = \text{MHL}$	21.25(2) ^b	17.53(7)
2	$\text{M} + \text{L} = \text{ML}$	17.43(1)	12.50(1)
3	$\text{M} + \text{L} + \text{H}_2\text{O} = \text{ML}(\text{OH}) + \text{H}$	8.49(2)	2.62(2)
4	$\text{ML} + \text{H} = \text{MHL}$	3.8	5.0
5	$\text{ML} + \text{H}_2\text{O} = \text{ML}(\text{OH}) + \text{H}$	-8.9	-9.9

^a Charges omitted for clarity. ^b Values in parentheses are standard deviations in the last significant figure.

formation of the $[\text{CuL}]^{2+}$ complex by the 2:2 pyridinophane **L2** is $\log K_{\text{ML}/\text{M-L}} = 20.90$, which is very close to the value we have obtained for **L** (Table 3, entry 4). If we compare with **L1** (Table 4), the tripodal synthon used for the preparation of **L**, the value obtained in this case ($\log K_{\text{ML}/\text{M-L}} = 17.42$) is lower than for **L1** and for **L2**. Nevertheless, it has to be emphasized that these ligands have donor atoms with different characteristics. **L1** has two primary nitrogen donors that display σ -donating abilities different from those of the secondary nitrogens in the bridges of **L** or **L2**. Comparisons with other related tetraamines or pentaamines also point in the same direction.^{21,26,27} Thereby, all these data suggest a coordination number of 4 as likely for the mononuclear complexes of **L**, although the participation of another nitrogen occupying a distorted axial position cannot be ruled out.

In this respect, one point of interest regards whether the atoms in the dangling arms are coordinated to the metal ion or not. To have some more light about this point, we have recorded the UV-vis spectra at pH values corresponding with the protonated $[\text{Cu}(\text{H}_x\text{L})]^{(2+x)}$ and neutral $[\text{CuL}]^{2+}$ species. The spectra do not experience significant variations for the different species and suggest that there are not important changes in the coordination environment although they are rather uninformative. The observed changes in the UV region of the spectra are also meaningless.

(25) de Silva, A. P.; Gunaratne, H. Q. N.; Coy, C. P. M. *Chem. Commun.* **1996**, 2399.

(26) Rothermel, G. L., Jr.; Miao, L.; Hill, A. L.; Jackels, S. C. *Inorg. Chem.* **1992**, *31*, 4854.

(27) Basallote, M. G.; Durán, J.; Fernández-Trujillo, J.; Mánuez, M. A.; Quirós, M.; Salas, J. M. *Polyhedron*. **2001**, *20*, 297.

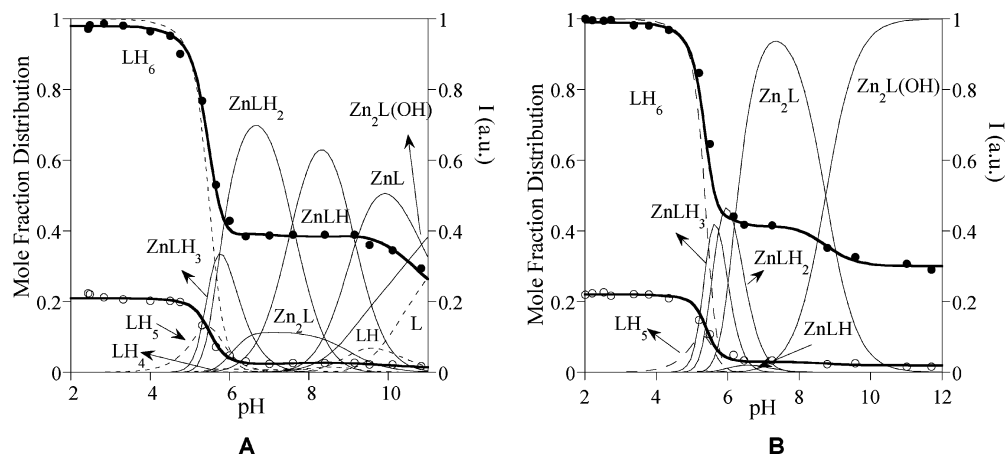


Figure 3. Steady-state fluorescence emission titration curves for the system $\text{Zn}^{2+}-\text{L}$ ($\lambda_{\text{exc}} = 280 \text{ nm}$) for a $1.00 \times 10^{-5} \text{ M}$ of **L** (molar ratio 1:1 **L**:**M** (A) and 1:2 **L**:**M** (B)), with 0.15 M NaCl at 298.1 K in water: (●) emission followed at 323 nm (monomer); (○) excimer emission followed at 400 nm ; (free ligand dotted lines and metal complex solid lines) molar fraction distributions.

With respect to the formation of dinuclear complexes, Figure 2B shows that such species are predominant above $\text{pH} = 4$, where $[\text{Cu}(\text{H}_2\text{L})]^{5+}$ starts to prevail in solution. It is interesting to emphasize that the entry of the second metal ion is characterized by a much lower stability constant than the binding of the first metal ion (entries 4 and 17 in Table 3, $\log K_{\text{CuL}/\text{Cu}^+} = 20.13(9)$ and $\log K_{\text{Cu}_2\text{L}/\text{CuL}\cdot\text{Cu}} = 10.9$, respectively). This large reduction in stability has to be related to energy consumption due to macrocycle reorganization associated with the binding of the second metal ion. Cu_2L^{4+} experiences two hydroxylation steps which have very similar and rather high pK_a values ($\log K_{\text{Cu}_2\text{L}/\text{Cu}_2\text{L}(\text{OH})\cdot\text{H}} = -9.9$ and $\log K_{\text{Cu}_2\text{L}(\text{OH})/\text{Cu}_2\text{L}(\text{OH})_2\cdot\text{H}} = -10.0$, respectively, entries 15 and 16 in Table 3) pointing out that they occur independently, namely, each in one of the two coordination sites, and that the hydroxo groups do not behave as bridging ligands.

The analysis of the stability data for the mononuclear complexes formed in the system $\text{Zn}^{2+}-\text{L}$ leads to similar conclusions as those of the $\text{Cu}^{2+}-\text{L}$ system. The value of the stability constant for the formation of the $[\text{ZnL}]^{2+}$ species is of the same order of magnitude as those available for other tetraamines such as 1,4,7,10-tetraazadecaamine (trien) ($\log K_{\text{ML}/\text{M}\cdot\text{L}} = 12.0$) and higher than those generally reported for triamines such as 1,4,7-triazaheptane ($\log K_{\text{ML}/\text{M}\cdot\text{L}} = 8.8$).²⁸ However, the obtained constant is clearly lower than that reported for the tripodal tetraamine tris(2-aminoethyl)amine (tren) ($\log K_{\text{ML}/\text{M}\cdot\text{L}} = 14.5$) or than the one we have obtained for **L1**, which also displays tripodal characteristics ($\log K_{\text{ML}/\text{M}\cdot\text{L}} = 12.50$, Table 4). The topology of the latter ligands favors a tetrahedral coordination geometry, in which the Zn^{2+} feels at ease due to the absence of ligand field stabilization of this metal ion. Therefore, although in the case of Zn^{2+} the differences in the constants are not so relevant due to the full subshell of this metal ion, 4 seems to be a likely coordination number for the mononuclear complexes. The protonation constants of $[\text{ZnL}]^{2+}$ shown in Table 3 (entries 10–12) indicate that these processes take place in noncoordinated nitrogen atoms.

With respect to the binding of a second Zn^{2+} ion to give dinuclear complexes, the first point to be noticed is that, in this case, the reduction in the constant is much less sharp than in the case of Cu^{2+} (entries 4 and 17 in Table 3, $\log K_{\text{ZnL}/\text{Zn}^+} = 11.75(9)$ and $\log K_{\text{Zn}_2\text{L}/\text{ZnL}\cdot\text{Zn}} = 9.4$, respectively). A second point of interest is the formation of a dinuclear monohydroxo complex ($\text{pK}_a = -8.8$, entry 15) that is predominant in solution above $\text{pH} 9$ (Figure 3).

A final point of interest regards whether the nitrogen atoms in the bridge are involved, or not, in the coordination to the metal ion. Although the ^1H NMR spectra give rise to very broad signals denoting a fluxional behavior or/and to the presence of different conformations, a careful analysis of the $^1\text{H}-^1\text{H}$ COSY experiments gives some information at this respect. Indeed $^1\text{H}-^1\text{H}$ correlation experiments performed for the free ligand in the region $4.00-5.00 \text{ ppm}$ do not show any cross-peaks since either benzylic protons $\text{py}0$ or $\text{N}0$ (for the labeling, see Chart 1), which are the ones resonating at this frequencies, are magnetically equivalent. Addition of Zn^{2+} either in 1:1 or 2:1 molar ratio produces the loss of the magnetic equivalence of these methylene protons, and thereby cross-peaks are observed in this region. This observation indicates that the arms are somewhat blocked by the presence of the metal ions suggesting the involvement of the nitrogens in the arms in the coordination. However, the large number of peaks that appear supports again the existence of different conformations for the complexes including those in which the naphthyl nitrogen would not be involved in the coordination.

Steady-State Fluorescence Measurements. Figures 2A,B and 3A,B collect the fluorescence emission titration curves of **L** with Cu^{2+} and Zn^{2+} superimposed with the molar fraction distribution curves obtained by potentiometry (Figures 2A and 3A, molar ratio **M**:**L** 1:1; Figures 2B and 3B, molar ratio 2:1).

For the two metal ions, as above-mentioned, the absorption spectra of the complexes are very similar to those of the free ligand, consisting of a typical naphthalene band with maximum values at 262 , 271 , and 280 nm , and are slightly dependent on pH .

(28) Martell, A. E.; Smith, R. M.; Moteikaitis, R. J. *NIST Critical Stability Constants of Metal Complexes Database NIST Standard Reference Database*, version 4; NIST: Washington, DC, 1997.

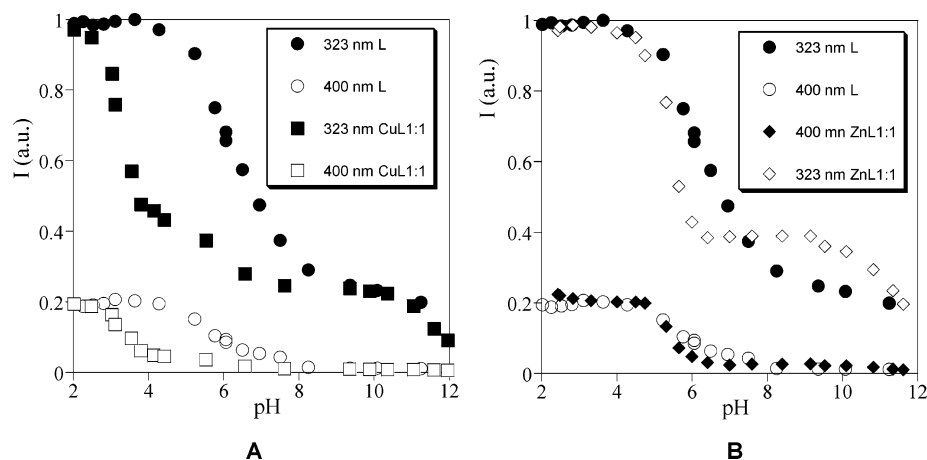


Figure 4. Fluorescence emission titration of **L** and in the presence of Cu(II) (A) and Zn(II) (B) in molar ratio 1:1 M:L.

Concerning the Cu^{2+} complexes, a strong CHEQ effect (*chelation enhancement of the quenching*)²⁹ can be observed in the pH range 3.0–5.5, in which the first complex species $[\text{Cu}(\text{H}_3\text{L})]^{5+}$ is formed.

In the titrations performed at M:L ratios 1:1, a partial quenching effect is observed for all species at neutral and alkaline pH values $[\text{Cu}(\text{H}_3\text{L})]^{3+}$, $[\text{Cu}(\text{H}_2\text{L})]^{2+}$, $[\text{Cu}(\text{HL})]^+$, and $[\text{CuL}]^{2+}$. In the titration carried out at 2:1 M:L molar ratio, a stronger quenching is observed for all the species presented in solution, namely $[\text{Cu}_2(\text{H}_2\text{L})]^{4+}$, $[\text{Cu}_2(\text{HL})]^{3+}$, $[\text{Cu}_2\text{L}]$, and the hydroxylated complexes $[\text{Cu}_2\text{L}(\text{OH})]^+$ and $[\text{Cu}_2\text{L}(\text{OH})_2]^+$. This quenching of the fluorescence emission upon Cu^{2+} complexation is commonly observed in polyamine ligands containing aromatic fluorophores and is attributed to an energy transfer quenching of the π^* emissive state through low-lying metal-centered states.⁵

In contrast with Cu^{2+} , the Zn^{2+} complexes of polyamine ligands are in generally emissive species leading to a CHEF effect (*chelation enhancement of the fluorescence emission*).^{5c,30} Comparison of the fluorescence emission titration curves, reported in Figures 1 and 4, shows that in this case a very modest CHEF effect is manifested for the monomer emission in the pH range 8–11. Concerning the excimer, coordination of **L** to Zn^{2+} breaks the interaction between the chromophoric units, leading to the disappearance of the excimer above pH = 6, Figure 3.

The naphthyl nitrogens, the closest to the fluorophoric units, are the most important in the electron-transfer quenching process that allows signaling the presence of protons and metal cations in polyamine systems.¹⁶ The stronger the involvement of these nitrogens in protonation and/or complexation, the stronger is the luminescence of the ligand. That is the reason complexation with Zn^{2+} is expected to produce a CHEF effect (Figure 3). On the other hand, protonated pyridine is known to quench anthracene fluorescence by a photoinduced electron-transfer mechanism²⁵ from the excited

anthracene to the pyridinium. Participation of the pyridine lone pair in Zn^{2+} complexation is expected to produce the same effect in the naphthalene emission. As a consequence, the expected CHEF arising from the involvement of the secondary amine lone pairs in metal ion complexation is compensated by CHEQ due to the complexed pyridine moiety.

For comparison purposes, steady-state fluorescence emission titrations were carried out in the absence and in the presence of Cu^{2+} and Zn^{2+} for the more flexible tripodal ligand **L1**, in which all four nitrogen atoms are involved in the coordination, Figures 5 and 6. In the system Cu^{2+} –**L1**, Cu^{2+} coordination produces a partial quenching of the emission in the pH range where the species $[\text{CuHL1}]^{3+}$ and $[\text{CuL1}]^{2+}$ exist. Formation of the monohydroxylated species $[\text{CuL1}(\text{OH})]^+$ induces complete quenching of the fluorescence. In the case of Zn^{2+} , a large CHEF effect is observed above pH = 6, Figure 6, that decreases upon hydroxylation of $[\text{ZnL1}]^{2+}$. While the CHEQ effect of Cu^{2+} is strong in both systems, the CHEF effect of Zn^{2+} with **L1** is much stronger than with **L**, once again confirming the quenching of naphthalene emission by the complexed pyridine moiety.

Fluorescence decays in the presence of metal ions were also measured. The fits are multiexponential, and the decay times and amplitudes are given as Supporting Information.

Conclusions

A novel bibrachial lariat aza-crown containing pyridine spacers and 2-((naphthylmethyl)amino)ethyl appendages has been prepared in good yield and its protonation behavior and Cu^{2+} and Zn^{2+} coordination chemistry studied by a variety of techniques.

The molecule presents different conformers as a function of pH. These ground-state conformers affect remarkably the emissive properties of the ligand. Steady-state fluorescence measurements show emissions due to the monomer and to excimer formed between the two naphthalene fragments of the macrocycle. The time-resolved fluorescence data and DOSY experiments show that a significant percentage of excimer is preformed as ground-state dimers.

Complexation of **L** with Cu^{2+} and Zn^{2+} shows the formation of mono- and dinuclear complexes in which the

(29) Alves, S.; Pina, F.; Albelda, M. T.; García-España, E.; Soriano, C.; Luis, S. V. *Eur. J. Inorg. Chem.* **2001**, 2, 405.

(30) (a) Valeur, B. *Molecular Fluorescence. Principles and Applications*; Wiley-VCH: Weinheim, Germany, 2002. (b) Bernardo, M. A.; Pina, F.; García-España, E.; LaTorre, J.; Luis, S. V.; Llinares, J. M.; Ramírez, J. A.; Soriano, C. *Inorg. Chem.* **1998**, 37, 3935.

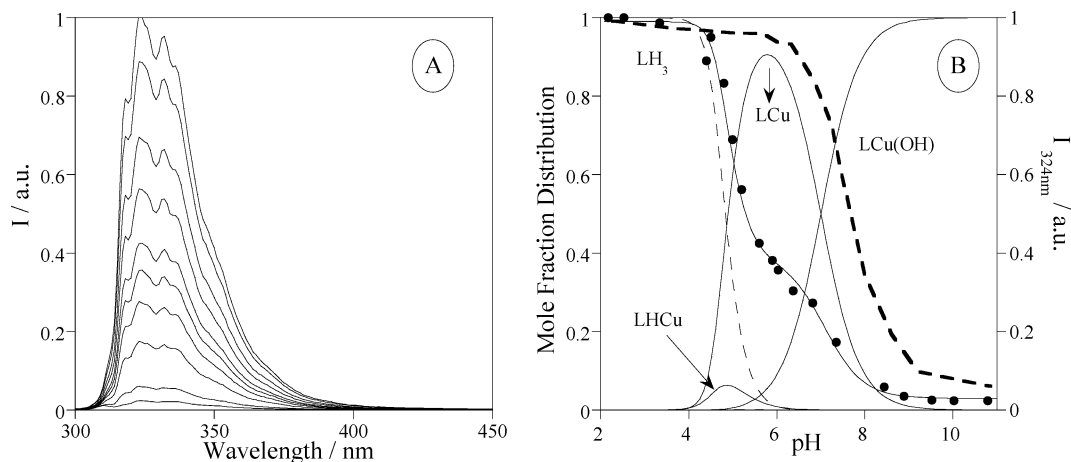


Figure 5. (A) Fluorescence emission spectra at excitation wavelength of 280 nm of the system Cu^{2+} -**L1** at 298.1 K. $[\text{Cu}^{2+}] = [\text{L1}] = 3.23 \times 10^{-5}$ M, in the presence of 0.15 M NaCl and at pH = 2.00, 4.32, 5.15, 5.40, 5.77, 6.03, 6.81, 7.60, 8.44, and 10.80. (B) Fluorescence emission spectra of the system Cu^{2+} -**L1** at 298.1 K ($\lambda_{\text{exc}} = 280$ nm, $\lambda_{\text{em}} = 324$ nm (●), $[\text{Cu}^{2+}] = [\text{L1}] = 3.23 \times 10^{-5}$ M, $[\text{NaCl}] = 0.15$ M), superimposed on the respective mole fraction distribution of the different species present in solution. Protonated curves are indicated by dashed lines, and complexed curves, by solid lines. In (B) is included the emission of the free ligand (black dotted bold lines).

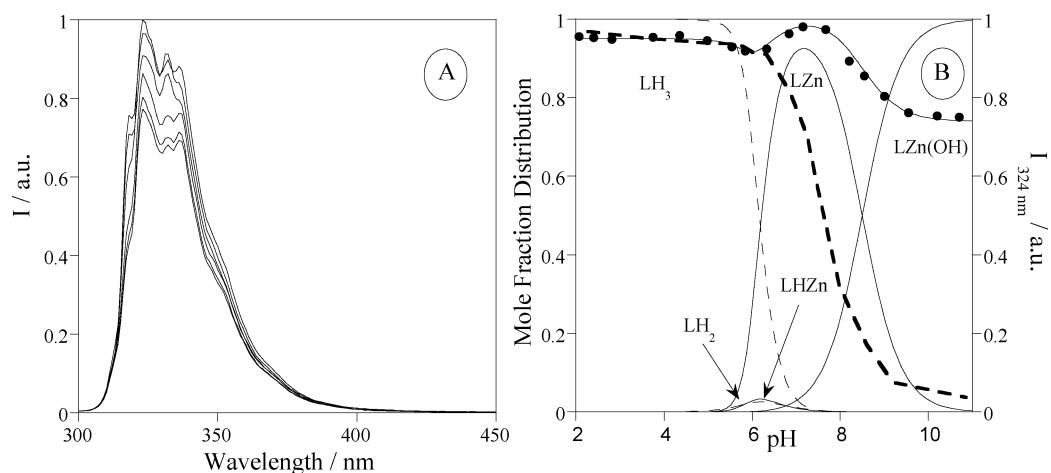


Figure 6. (A) Fluorescence emission spectra at excitation wavelength of 280 nm of the system Zn^{2+} -**L1** at 298.1 K in the presence of 0.15 M NaCl and pH = 2.07, 5.84, 7.15, 8.20, 9.00, and 10.70. (B) Fluorescence emission spectra of the system Zn^{2+} -**L1** at 298.1 K ($\lambda_{\text{exc}} = 280$ nm, $\lambda_{\text{em}} = 324$ nm (●), $[\text{Zn}^{2+}] = [\text{L1}] = 3.23 \times 10^{-5}$ M, $[\text{NaCl}] = 0.15$ M), superimposed on the respective mole fraction distribution of the different species present in solution. Protonated curves are indicated by dashed lines, and complexed curves, by solid lines. In (B) is included the emission of the free ligand (black dotted bold lines).

nitrogen atoms in the pendant arms do not provide a strong contribution to the overall stability. Cu^{2+} complexation gives rise to a CHEQ effect while Zn^{2+} originates a slight CHEF effect. The acid–base, coordination capabilities, and emissive behavior of **L** were compared with those presented by its synthetic precursor **L1**. The differences in fluorescence properties evidenced by their Zn^{2+} complexes support the existence of an electron-transfer quenching mechanism from excited naphthalene to complexed pyridine.

Acknowledgment. Financial support from the Generalitat Valenciana AVCYT (Spain), projects GV04B225 and GRUP03/198 Acciones Integradas Hispano-Portuguesas, project 32442/99 PRAXIS/QUI/10137/98 (Portugal), FEDER (Portugal), and European Community's Human Potential Program under contract HPRN-CT-2000-00029 (Molecular

Level Devices and Machines) is gratefully acknowledged. C.L. acknowledges a postdoctoral grant from contract HPRN-CT-2000-00029. R.A. acknowledges the MEC for a Ph.D. grant (AP2002-1382).

Supporting Information Available: Table S1, listing fluorescence decay times (τ_i) and preexponential factors (A_{ij}) as a function of pH for the metal:ligand (Zn:L , $\text{Zn}_2\text{:L}$, and Cu:L) complexes obtained with excitation wavelength of 285 nm and emission wavelengths of 320 and 420 nm, text discussing the results from Table 1, Figure S1, showing a DOSY experiment for **L** recorded at pD = 6.4, and a description of the experimental procedure of the DOSY measurements. This material is available free of charge via the Internet at <http://pubs.acs.org>.

IC049694T